



Methods for Three-Dimensional All-Optical Manipulation of Neural Circuits

*Emiliano Ronzitti, Valentina Emiliani and Eirini Papagiakoumou**

Wavefront Engineering Microscopy Group, Photonics Department, Institut de la Vision, Sorbonne Université, Inserm S968, CNRS UMR7210, Paris, France

Optical means for modulating and monitoring neuronal activity, have provided substantial insights to neurophysiology and toward our understanding of how the brain works. Optogenetic actuators, calcium or voltage imaging probes and other molecular tools, combined with advanced microscopies have allowed an “all-optical” readout and modulation of neural circuits. Completion of this remarkable work is evolving toward a three-dimensional (3D) manipulation of neural ensembles at a high spatiotemporal resolution. Recently, original optical methods have been proposed for both activating and monitoring neurons in a 3D space, mainly through optogenetic compounds. Here, we review these methods and anticipate possible combinations among them.

Keywords: light-shaping, three-dimensional photostimulation, three-dimensional functional imaging, all-optical neuronal studies, optogenetics, neural circuits

OPEN ACCESS

Edited by:

Marco Canepari,
UMR5588 Laboratoire
Interdisciplinaire de Physique (LIPhy),
France

Reviewed by:

Albrecht Stroh,
Johannes Gutenberg University
Mainz, Germany
Marco Lorenzo Dal Maschio,
Università degli Studi di Padova, Italy

*Correspondence:

Eirini Papagiakoumou
eirini.papagiakoumou@inserm.fr

Received: 04 September 2018

Accepted: 19 November 2018

Published: 17 December 2018

Citation:

Ronzitti E, Emiliani V and
Papagiakoumou E (2018) Methods
for Three-Dimensional All-Optical
Manipulation of Neural Circuits.
Front. Cell. Neurosci. 12:469.
doi: 10.3389/fncel.2018.00469

INTRODUCTION

Controlling and monitoring neuronal activity with a light has become a common practice in many neurobiological studies, throughout the last decade. The continuously expanding toolbox of molecular probes that activate/inhibit (Herlitze and Landmesser, 2007; Airan et al., 2009; Levitz et al., 2013; Klapoetke et al., 2014; Shemesh et al., 2017; Becker et al., 2018; Guruge et al., 2018; Mardinly et al., 2018) or image (Emiliani et al., 2015; Kim et al., 2018) neuronal activity as well as the development of original light-microscopy methods for stimulating these tools (Ronzitti et al., 2017b; Chen et al., 2018c; Yang and Yuste, 2018), has tremendously contributed to the direction of research and has led to innovative experimental concepts (Rickgauer et al., 2014; Carrillo-reid et al., 2016). Photostimulation via optogenetics and/or uncaging (Kwon et al., 2017) is suitable for single cell and, most importantly, circuit studies, since light gives access to a large number of targets simultaneously, at high spatial precision via parallel illumination methods (Papagiakoumou et al., 2010; Packer et al., 2015; Forli et al., 2018; Yang et al., 2018).

Circuit studies are usually performed *in vivo* by light-stimulation at near-infrared to minimize scattering effects and optimize spatial resolution via non-linear multiphoton absorption processes. Ideally, these studies also demand three-dimensional (3D) accessibility both for activation and imaging at physiological time scales (few-ms scale activation and imaging). 3D imaging approaches enable the use of complementary strategies to access volumes extending up to a few hundred μm s in the axial direction, by proposing the use of piezo scanners to scan the objectives in specific trajectories (Göbel et al., 2007), acousto-optic deflectors (Reddy et al., 2008; Grewe et al., 2010; Katona et al., 2012; Nadella et al., 2016), tunable lenses (Grewe et al., 2011; Fahrbach et al., 2013; Kong et al., 2015), spatiotemporal multiplexing (Cheng et al., 2011; Ducros et al., 2013), light field

microscopy (Prevedel et al., 2014), or Bessel beam excitation (Lu et al., 2017) and reaching tens of Hz imaging frequencies, of neuronal activity *in vivo* (Göbel et al., 2007; Grewe et al., 2011; Katona et al., 2012; Nadella et al., 2016). 3D functional imaging of neurons has more recently been demonstrated at even larger volumes, reaching 0.5 mm in *z*, using a temporally focused Gaussian beam excitation at the size of neuron soma (Prevedel et al., 2016), with large field views up to 5 mm in *xy* (Sofroniew et al., 2016; Stirman et al., 2016) or in two different areas of the brain (Lecoq et al., 2014; Chen et al., 2016).

The development of 3D photoactivation methods is more recent. These systems are based on the use of Computer-Generated Holography (CGH) (Papagiakoumou et al., 2018; Yang and Yuste, 2018). Although this technique was established for the projection of 3D patterns (Piestun et al., 1996; Haist et al., 1997) or diffraction-limited spots (Liesener et al., 2000) via spatial light modulators (SLMs) several years ago, its use in neuroscience for simultaneous activation of multiple targets in two (Lutz et al., 2008; Nikolenko et al., 2008; Dal Maschio et al., 2010) or three dimensions (Yang et al., 2011; Go et al., 2012; Hernandez et al., 2016; Dal Maschio et al., 2017) was established only during the last decade. Thanks to 3D-CGH, used either solely (parallel methods) or in its diffraction-limit version in combination with scanning of the holographic beamlets (hybrid methods) [see (Papagiakoumou, 2013; Ronzitti et al., 2017b) for detailed description of these approaches], it is possible nowadays to activate multiple neurons providing both the adequate temporal resolution, as well as the spatial resolution for single-cell precision (Figures 1A,B).

With regards to temporal resolution, it is helpful to define the notion of *temporal precision* in optogenetic activation, i.e., the degree of reproducibility of the occurrence timing of a photo-evoked AP (also indicated as photo-evoked spike jitter) (Figure 1C) and *temporal resolution*, i.e., the time needed to photo-evolve an AP, ultimately linked to the maximum achievable light-driven neuronal firing rate (Figure 1D). Minimizing those two parameters helps to reproduce precise temporal patterns of activity that in combination with multicell activation, enables to mimic the physiological activity of a network. It has been shown that parallel photoactivation methods (Ronzitti et al., 2017b) can easily achieve short timescales during optogenetic activation (few-ms temporal resolution and sub-ms jitter) (Chaigneau et al., 2016; Ronzitti et al., 2017a; Shemesh et al., 2017; Chen et al., 2018b). Later studies using scanning methods, have also shown a high temporal specificity, reaching a millisecond jitter by using high power in the excitation spots (Yang et al., 2018).

With regards to 3D spatial resolution, scanning methods using 3D-CGH show an intrinsically good spatial resolution, thanks to the small spot size of the excitation beam (close to diffraction limit). Nevertheless, resolution can dramatically decrease when using intensities close to the saturation levels for the opsin, which results in out-of-focus excitation (Rickgauer and Tank, 2009; Andrasfalvy et al., 2010). Parallel methods use illumination shapes that cover the whole cell body, in order to achieve parallel recruitment of all opsins on the cell membrane to improve efficiency (Papagiakoumou et al., 2010). This, however, causes a quick deterioration of the axial resolution, which scales linearly

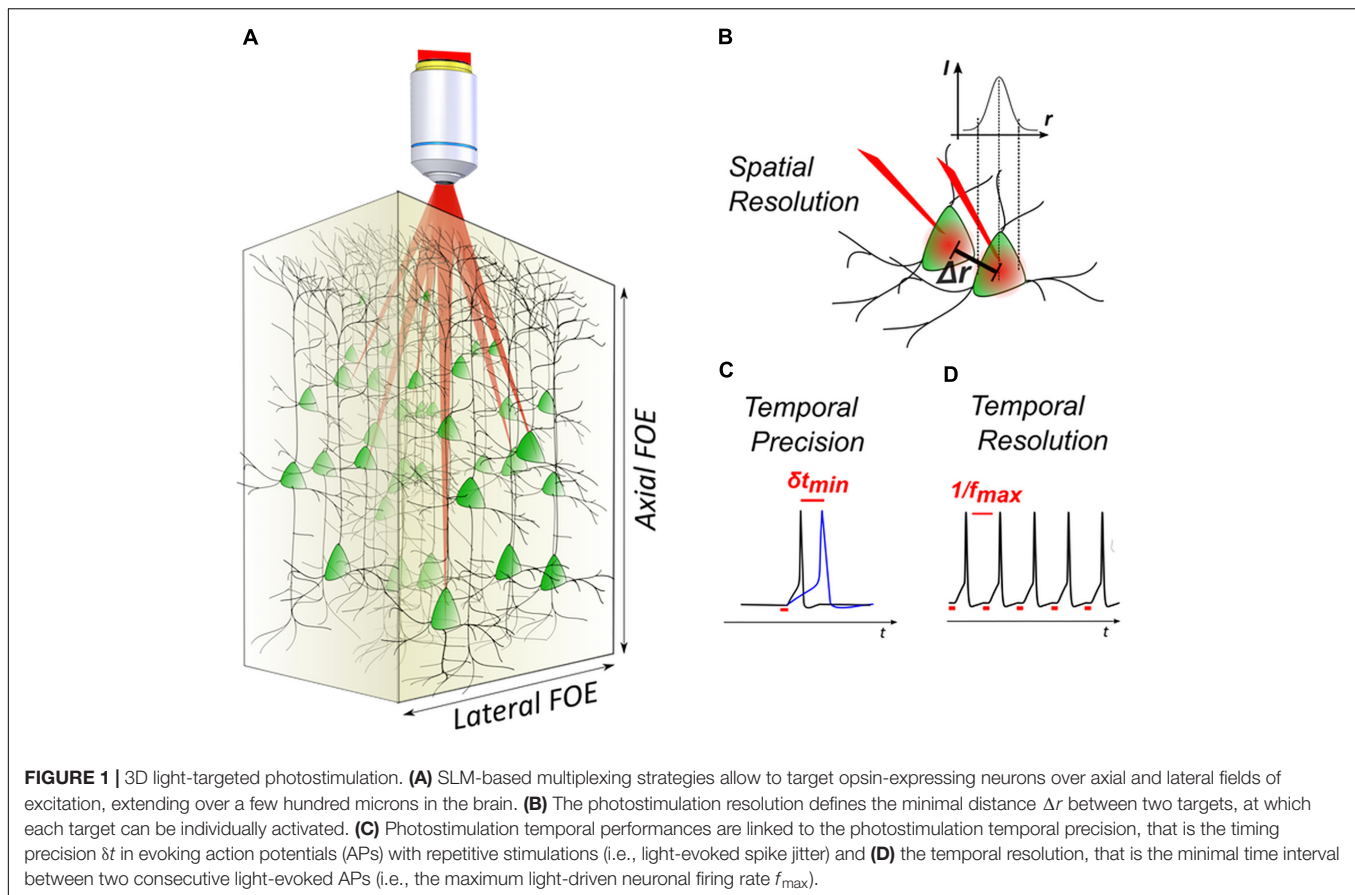
or quadratically with lateral size, for holographic or Gaussian beams, respectively (Oron et al., 2012). Parallel methods can provide a good axial resolution when combined with temporal focusing (TF) (Papagiakoumou et al., 2008, 2010; Oron et al., 2012; Rickgauer et al., 2014). Notably, temporally focused light-shaping methods allow to preserve sharp borders of the excitation pattern (Papagiakoumou et al., 2010), even through scattering media (Bègue et al., 2013; Papagiakoumou et al., 2013). However, because TF works by dispersing the spectral frequencies of a femtosecond light pulse at a specific plane (Oron et al., 2005), special configurations are needed to extend the methods in 3D.

Here we review the methods proposed so far for 3D photoactivation and present the possibilities for combination with 3D imaging modalities, to establish precise and flexible microscopy methods for all-optical manipulation of neural circuits. The methods we present here have mostly been developed for optogenetic photostimulation but in principle, any other photoactivation technique, such as uncaging of caged neurotransmitters, or activation of photoactivable proteins, could benefit from them.

ALL-OPTICAL MANIPULATION

The very first experiment of all-optical manipulation of neurons was demonstrated by activating cells in neocortical slices via two-photon (2P) uncaging of MNI-glutamate with multiple beamlets generated with a diffractive optical element, or one single beam multiplexed in time, and 2P Ca²⁺ imaging (Nikolenko et al., 2007). Similarly, a few years later in two other papers researchers measured Ca²⁺ signals in neurons while uncaging MNI-glutamate (Dal Maschio et al., 2010; Anselmi et al., 2011). In (Dal Maschio et al., 2010) the optical system incorporated 2P 2D-CGH in the optical path of a commercial 2P scanning microscope and it could exchange holographic or scanning stimulation between the uncaging and imaging beams. In (Anselmi et al., 2011) 3D-CGH with diffraction-limited spots was combined with a remote-focusing system (Botcherby et al., 2007, 2012) to perform functional imaging along tilted dendrites of hippocampal pyramidal neurons in brain slices. Although the first demonstrations of combined activation and imaging of neurons used uncaging, the term *all-optical* is mostly related to the combination of functional imaging and optogenetic activation. In 2014, a milestone was achieved when an important number of scientific studies showing the activation of neurons *in vivo* in rodents via optogenetic molecules and the imaging of Ca²⁺ responses with GCaMP, took place (Vogt, 2015), using either visible (Szabo et al., 2014) or 2P light stimulation (Rickgauer et al., 2014; Packer et al., 2015). More publications followed, using 2D (Carroll et al., 2015; Carrillo-reid et al., 2016; Bovetti et al., 2017; Förster et al., 2017; Forli et al., 2018), and more recently 3D stimulation (Hernandez et al., 2016; Dal Maschio et al., 2017; Mardinly et al., 2018; Yang et al., 2018).

Despite these very important studies, full optical neuronal control remains a challenge in terms of achieving reliable delivery and expression of sensors and actuators in the same neurons, eliminating the cross-talk between imaging and activation,



and recording and stimulating with a single-neuron and a single-action-potential precision (Emiliani et al., 2015). These problems have been discussed exhaustively in other recent reviews (Emiliani et al., 2015; Ronzitti et al., 2017b; Chen et al., 2018c). Here we will focus on reviewing the recent developments for 3D all-optical manipulation.

3D Photoactivation Fully Parallel Methods

Fully parallel optical methods proposed for 3D activation in an all-optical configuration have been presented for optogenetics and make use of extended light-pattern formation to cover the entire neuron soma. Light-patterns can be either large Gaussian beams generated by underfilling the objective numerical aperture (NA; low-NA Gaussian beams), or beams created with more flexible light-patterning methods such as CGH, generalized phase contrast (GPC) or amplitude modulation. As already mentioned, the limit of extended light patterns is the deterioration of the axial confinement, an issue that can be solved by using temporal focusing. Common experimental configurations of TF make use of a diffraction grating in a plane conjugate to the focal plane of the microscope objective (image formation plane), separating the spectral frequencies of the laser femtosecond pulses (dispersion of different wavelengths in different angles) (Oron et al., 2005; Zhu et al., 2005). In other words, the image projected at the grating plane is the image formed at the sample plane, while

2P absorption of light projected in any other plane before or after the grating, as it is the case when you generate a 3D pattern distribution, will be strongly weakened by the pulse broadening. This has, until recently, limited TF-light shaping to 2D configurations. Methods have been proposed for axial displacement of the TF plane for Gaussian beams, by introducing group velocity dispersion (Durst et al., 2006, 2008; Dana and Shoham, 2012). However, they are only suitable for remotely displacing one plane and they are not compatible with light-patterning techniques (Leshem et al., 2014), as they can displace the TF plane but not the spatial focusing one.

Hernandez et al. (2016) solved the problem, by introducing the axial displacement mechanism after the grating for TF, which decoupled lateral light shaping from axial displacements. The system used a conventional 2D-CGH with TF for lateral light-patterning and a second SLM placed at a Fourier plane after the grating to introduce the desired axial shift from the original focal plane, via a lens-effect phase modulation. This configuration also enabled the generation of different excitation patterns at distinct axial planes, by addressing the two SLMs in multiple regions, tiled vertically to the direction of dispersion for TF. With this configuration, researchers demonstrated for the first time the generation of multi-plane temporally focused patterns, reaching a volume of $240 \times 240 \times 260 \mu\text{m}^3$ with the axial confinement varying from $5 \mu\text{m}$ Full Width Half Maximum (FWHM) at the center of the field of excitation (FOE) to $10 \mu\text{m}$ at the edges

of it, tested with spots of 20 μm in diameter. The number of regions equal to the number of planes to be addressed. The system was used for selective 2P 3D photoconversion of the Kaede protein (Isobe et al., 2010) in the brain of zebrafish larvae (photoconversion at 800 nm with 0.1–4.0 $\text{mW}/\mu\text{m}^2$ depending the illumination duration) and for 2D optogenetic activation of ChR2 in zebrafish spinal cord neurons co-expressing GCaMP5G (excitation at 900 nm with 0.6 $\text{mW}/\mu\text{m}^2$). Monitoring of Ca^{2+} traces in that case was performed with visible illumination and two-color HiLo imaging (Lim et al., 2008) (at $\sim 30.8 \mu\text{W}/\text{mm}^2$).

Despite the flexibility of this system, an inherent limitation occurs in the maximum number of axial planes that could be addressed because of the physical tiling of the SLMs, before the quality of the holographic spots get distorted (~ 6 planes) (Hernandez et al., 2016). Although this can be sufficient for a number of biological applications (Yang et al., 2016), three new studies, have recently proposed ways to increase both the number of planes and the FOE. They all used the same principle: having a beam-shaping method for creating a 2D temporally focused pattern and using a SLM at a Fourier plane of the TF system for lateral and axial multiplexing of this pattern in several positions in 3Ds via 3D-CGH (**Figure 2A**). 3D-CGH is used to generate arrays of 3D diffraction-limited spots, using variations of the Gerchberg-Saxton algorithm (Gerchberg and Saxton, 1972; Di Leonardo et al., 2007) to calculate the phase profile to address to the SLM.

In two of these works the light-shaping part is a TF-Gaussian beam (Pégard et al., 2017; Sun et al., 2018) (**Figure 2B**). In (Pégard et al., 2017) 3D scanless holographic optogenetics with temporal focusing (3D-SHOT) was used to generate a large number of temporally focused spots, each of them fitting the size of a cell soma of pyramidal neurons (i.e., ~ 10 – $15 \mu\text{m}$ FWHM lateral size). With this approach, researchers reported the possibility to project hundreds of excitation spots in a total volume of $350 \times 350 \times 280 \mu\text{m}^3$. (Sun et al., 2018) presented a very similar approach as the one presented by (Pégard et al., 2017), using a TF experimental configuration with two gratings instead of a single grating and a lens. The beam's lateral size was 2.5 μm in diameter and the axial FWHM of the 2P light intensity was 7.5 μm . This study did not include any biological demonstration. The authors used the generated spots in direct laser writing inside a glass, which relies on non-linear light absorption at the focus. Fabrication was conducted either on the surface or inside standard microscope glass slides. As a novelty, they showed that they were able to place focal points at high lateral proximity (4 μm) with minimal interference between them. That is thanks to the pulse front tilt effect, a property inherent to TF systems where the arrival time of an ultrashort pulse in a certain plane varies across the beam profile thus creating a tilt between the pulse front and the direction perpendicular to the beam. In this way, adjacent spots can be spatially overlapped (Sun et al., 2018).

Both of these studies use Gaussian beams, which is technically simpler compared to the 3D-CGH-TF system proposed by (Hernandez et al., 2016). However, a considerable drawback of this system is the fact that the laser beam is focused on a line on the SLM used for 3D multiplexing, where the size depends on the linear dispersion of the TF system in the direction of dispersing

the spectral frequencies (usually parallel to the optical table), and it equals the monochromatic beam size in the unchirped dimension (vertical to the dispersion direction). In the chirped direction, care is usually given to fill the size of the SLM liquid crystal array, while in the unchirped direction the size of the beam is a few millimeters (2–3 mm) (Durst et al., 2008; Sun et al., 2018). This imposes a restriction to the maximum laser power used before damaging the SLM (and thus to the maximum number of spots that can be projected). To overcome this limitation Pégard et al. (2017) proposed adding an extra lens before dispersing the ultrashort pulses on the TF grating, defocusing the beam on the SLM and thus increasing the illumination area. Nevertheless, the defocusing created a secondary spatial focus in the form of a line that deteriorated the axial propagation of the beam (Pégard et al., 2017; Chen et al., 2018c). In a more advanced version of this method the lens was replaced by a rotating diffuser at an image plane, after the grating. This led to an enlarged illumination of the SLM, without secondary focus effects (Mardinly et al., 2018) and Gaussian beams of 23 μm axial FWHM (axial optical Point Spread Function; PSF) (Pégard et al., 2018). 3D-SHOT was used in this case to simultaneously stimulate neurons co-expressing newly developed excitatory or inhibitory somatic opsins, ST-ChroME or IRES-ST-eGTACR1, respectively, and GCaMP6s in an all-optical configuration (about 50 neurons in three different planes extending to an axial range of 100 μm , 0.13 $\text{mW}/\mu\text{m}^2$ or 40 mW per target for activating ST-ChroME neurons, 0.08 $\text{mW}/\mu\text{m}^2$ or $\sim 6 \text{mW}$ per target for IRES-ST-eGTACR1 neurons, illumination with a low-repetition rate laser at 1040 nm for 1 s) (Mardinly et al., 2018).

Higher flexibility and better axial resolution was demonstrated by Accanto et al. who presented a system for multiplexed temporally focused-light shaping (MTF-light shaping), where the beam-shaping part was either 2D-CGH or GPC (Accanto et al., 2018) (**Figure 2C,D**). For MTF-CGH, the optical setup is the same as the one of 3D-CGH-TF (Hernandez et al., 2016), the only difference being the way the multiplexing SLM is addressed. MTF-CGH enabled investigators to generate 15- μm diameter temporally focused holographic spots on 50 independent planes on an excitation field of $300 \times 300 \times 500 \mu\text{m}^3$ and an average axial PSF of 11 μm FWHM. The theoretical FOE for the optical parameters they used was $750 \times 750 \times 990 \mu\text{m}^3$, but was experimentally limited by the size of the optics used.

In MTF-GPC the beam-shaping part was substituted by a GPC setup (Glückstad, 1996; Papagiakoumou et al., 2010) for projection of high-precision, speckle-less, temporally focused arbitrarily shaped patterns. Notably, the combination of GPC with CGH to extend GPC to 3D was previously reported (Go et al., 2011; Bañas and Glückstad, 2017) but without TF, which is essential for suppressing excitation by the out-of-focus light (Papagiakoumou et al., 2010). In MTF-GPC, characterization of 12- μm diameter TF-GPC spots showed improved axial PSF, compared to MTF-CGH (6 μm FWHM on average on a FOE of $200 \times 200 \times 200 \mu\text{m}^3$), as expected for TF-GPC patterns (Papagiakoumou et al., 2010). Similar to the Gaussian beam case, a crucial drawback remains the illumination of the multiplexing SLM with a line. To overcome this, (Accanto et al., 2018) removed the phase contrast filter and used the first SLM of their

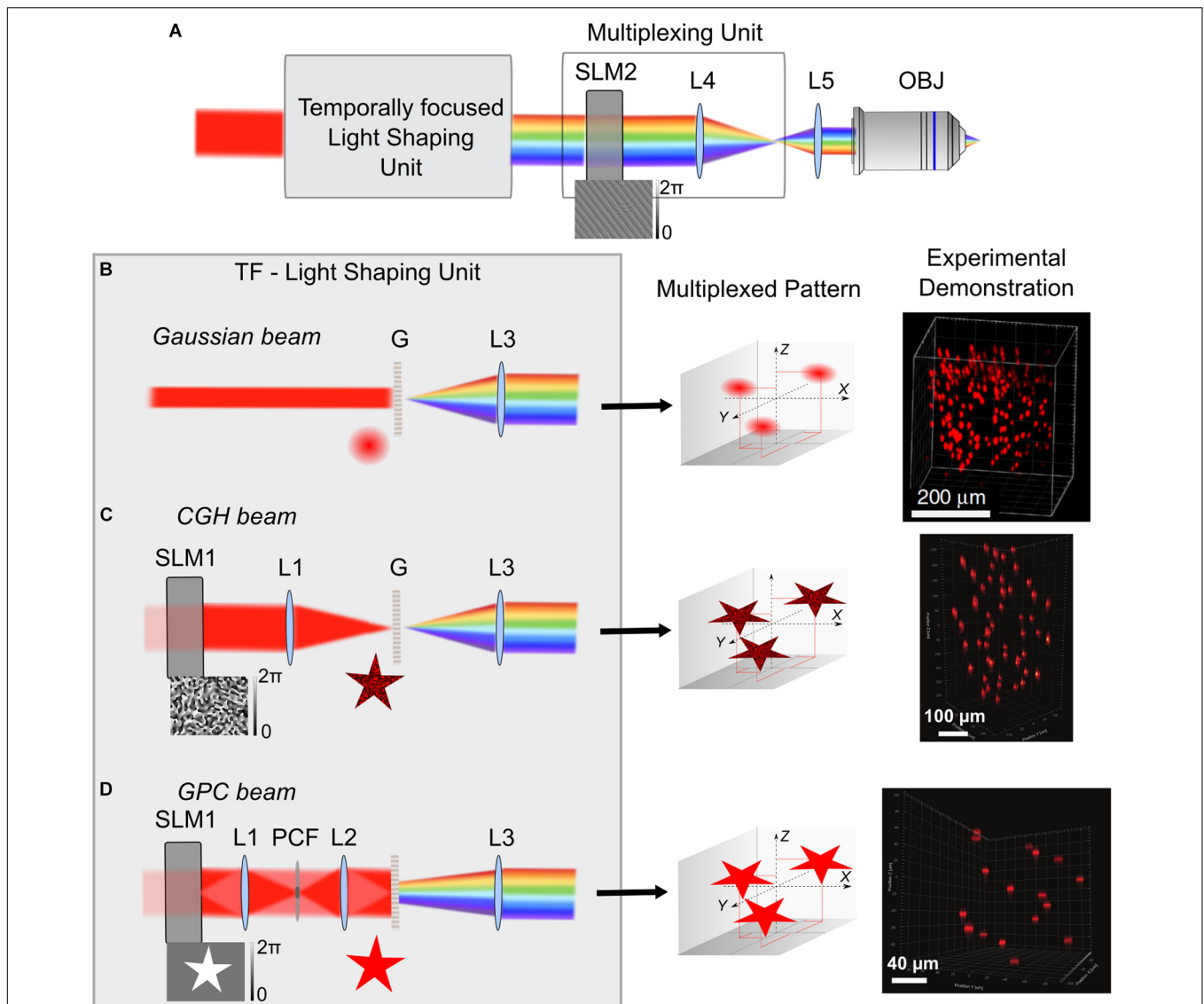
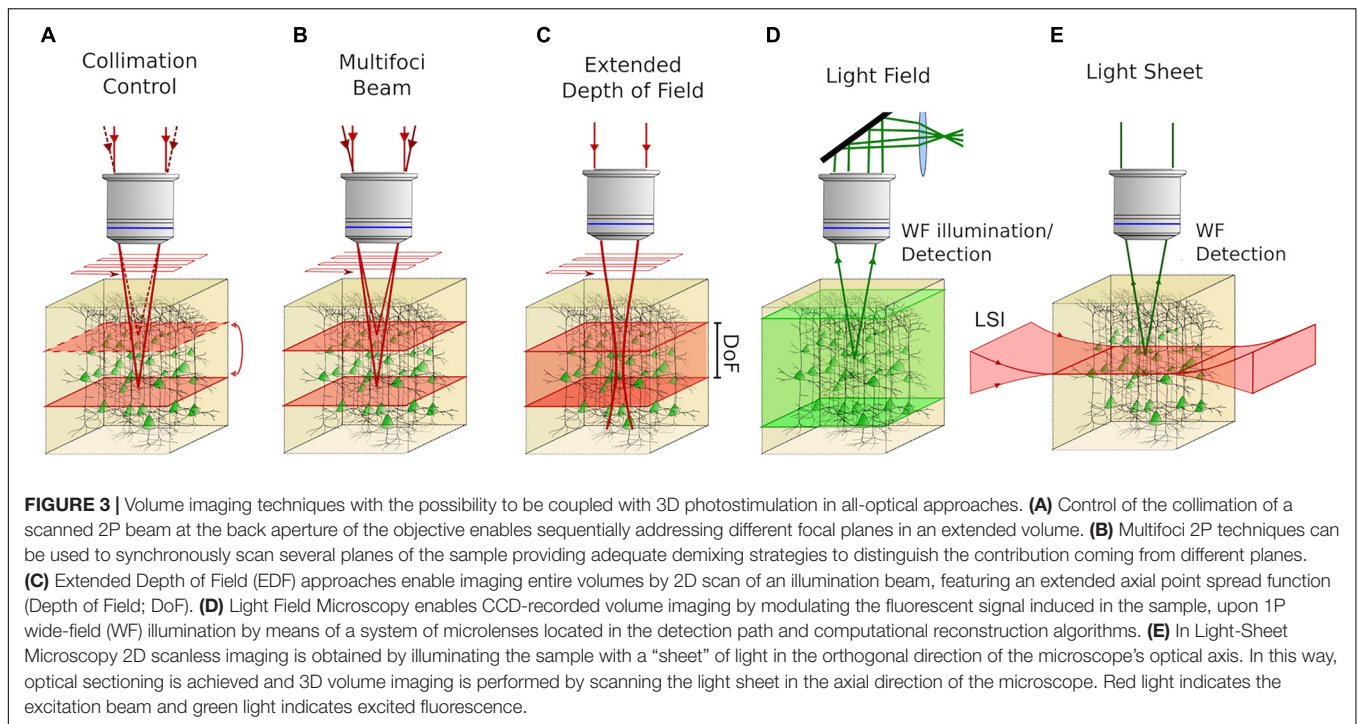


FIGURE 2 | 3D multiplexed temporally focused light shaping. **(A)** Optical systems for 3D temporally focused light shaping consist of a light-shaping unit for creating a 2D temporally focused pattern and a multiplexing unit, using a SLM (SLM2) at a Fourier plane of the TF system, to replicate the 2D pattern in several positions in 3D via 3D-CGH (example of a phase profile for projecting 3 diffraction-limited spots in different positions on the bottom of SLM2). After the light-shaping unit, the beam is represented with its spectral frequencies diffracted, because of spectral diffraction by the grating G. After phase modulation on SLM2 the beam is imaged by two lenses (here L4 and L5) to the back aperture of the microscope objective. **(B–D)** Different cases for the TF-light-shaping unit: **(B)** Gaussian beam. In this case the grating is illuminated with a collimated Gaussian beam of a suitable size, usually adjusted with a telescope of lenses (not shown here). Configuration with a non-collimated beam (by introducing a lens prior to the grating) was used by Pégard et al. (2017) in order to increase the illuminated area of SLM2. Middle. Illustration of the example for projection of 3 Gaussian replicas, when the SLM2 is illuminated with the phase profile shown in **A**. Right. Experimental demonstration showing projection of 200 Gaussian beams in a $350 \times 350 \times 280 \mu\text{m}^3$ volume, adapted from Pégard et al. (2017). **(C)** CGH beam. A SLM (SLM1) and a lens (L1) are used for holographic pattern projection (here, a star), that is then replicated in the 3 different positions (Middle). Right. Experimental demonstration of 50 holographic circular spots of $15 \mu\text{m}$ diameter in a $300 \times 300 \times 500 \mu\text{m}^3$ volume, adapted from Accanto et al. (2018). **(D)** GPC beam. SLM1 is used for a binary phase modulation of $\Delta\varphi = \pi$, that is then phase contrasted by the phase contrast filter (PCF), placed at the focal plane of L1. A sharp speckle-free pattern is formed at the grating plane by L2. Middle. 3 replicas for the GPC pattern in the corresponding predefined positions of the multiplexing unit. Right. Experimental demonstration of projection of 17, $12\text{-}\mu\text{m}$ diameter circular GPC spots in a $200 \times 200 \times 200 \mu\text{m}^3$ volume, adapted from Accanto et al. (2018). L3 Collimating lens.

configuration to perform amplitude and phase modulation. They encoded a pattern in four different areas on the beam-shaping SLM and the pattern of each area was laterally displaced with a different prism-phase effect, such as generating four different lines on the multiplexing SLM after the beams were temporally

focused. Addressing the first SLM in different areas enabled the projection of replicas of four different speckle-free patterns in a volume of $300 \times 300 \times 400 \mu\text{m}^3$, a method referred to as MTF-Multi Shapes. This strategy both increased the illumination area of the multiplexing SLM and allowed more flexibility on



the shape of the projected patterns, similar to that described by (Hernandez et al., 2016).

Evidently, flexibility of the MTF-light shaping methods comes at the cost of simplicity of the optical setup and total cost. For simpler cost-effective solutions in applications where the excitation spot size and form can be predetermined, it is possible to use static lithographically fabricated phase masks (Accanto et al., 2018) to replace the first SLM in MTF-CGH, or a GPC-light shaper (Bañas et al., 2014) to replace the GPC setup in MTF-GPC.

MTF-CGH was used in a multi-cell excitation of photoactivatable GCaMP (paGCaMP) in the central nervous system of the drosophila larvae (photoconversion at 760 nm with $1.0 \text{ mW}/\mu\text{m}^2$, illumination with trains of 10-ms pulses at 50 Hz, total illumination duration: tens of seconds up to 4 min) and to photoconvert Kaede in the zebrafish larva hindbrain (photoconversion at 800 nm with $0.4 \text{ mW}/\mu\text{m}^2$, illumination with trains of 10-ms pulses at 50 Hz, total illumination duration 1–4 min). Parallel illumination of neurons allowed fast photoconversion in both cases, with minimal photoactivation of untargeted neighboring cells. Especially in the case of paGCaMP, neuronal processes of the targeted cells could be clearly distinguished from the background, allowing the possibility to precisely track neuronal morphology (Accanto et al., 2018).

Although the use of TF in neuronal photoactivation with parallel methods has offered the possibility to locally confine the excitation volume, such as to preserve single-cell resolution, this might not be necessary for low-scattering samples, excitation of small size cells or sparse staining. In that case, 3D-CGH alone can be used for the projection of extended light patterns in different planes (Haist et al., 1997; Hernandez et al., 2016). Thus 2P 3D-CGH spots of $6\text{-}\mu\text{m}$ diameter were used to photoactivate Chr2 in the zebrafish larval neurons, which in

combination with 2P GCaMP6s Ca^{2+} imaging, enabled the identification of neuronal ensembles associated with control of tail bending (photoactivation at 920 nm, $0.2 \text{ mW}/\mu\text{m}^2$ or 50 mW per target, circular overlapping photoactivation regions of $18 \mu\text{m}$ in diameter) (Dal Maschio et al., 2017). Moreover, the authors performed targeted photoactivatable GFP (paGFP) photoconversion to obtain a morphological reconstruction of individual functionally identified neurons (photoconversion at 750 nm with $0.25 \text{ mW}/\mu\text{m}^2$ or 7 mW per target, 1-s illumination).

Finally, as a general comment we should note that 3D-TF methods using CGH for multiplexing the excitation spot, can produce powerful experimental configurations in volumetric FOEs, with the quality of all spots being the same across the whole FOE, since the spots multiplexed are replicas of the same single original spot. However, for volumes reaching mm-range, care should be taken to homogenize the excitation properties of the projected spots, by taking into account factors such as scattering with increasing depth, SLM-diffraction-efficiency corrections, optical aberrations due to the large defocusing of spots (objective used at its limits) or projection near the borders of the FOE, and spectral aberrations for TF occurring by cropping spectral frequencies in the optics when using large defocus (Hernandez et al., 2016).

Hybrid Methods

Scanning methods are alternative approaches for neuronal stimulation and have been widely used in 2P optogenetics (Rickgauer and Tank, 2009; Andrasfalvy et al., 2010; Packer et al., 2012; Prakash et al., 2012), mainly for the activation of the slow kinetics opsin, CIV1, and most of the times in a spiral trajectory (Packer et al., 2012, 2015; Carrillo-reid et al.,

2016; Yang et al., 2018). They represent the simplest and most immediate solution for many laboratories, since they adopt conventional 2P scanning microscopes based on galvanometric scanners. Nevertheless, the sequential photostimulation limits the achievable temporal resolution (Papagiakoumou, 2013; Ronzitti et al., 2017b) and does not allow the simultaneous activation of multiple targets. The use of resonant scanners or acousto-optic deflectors (AODs) to increase the temporal resolution of scanning methods, is still limited by the necessary dwell time in 2P excitation, especially for slow opsins (Prakash et al., 2012). Moreover, due to their cycling at resonant frequencies (8 kHz), resonant scanners cannot provide the necessary flexibility for arbitrary excitation trajectories, like spiral scans. For simultaneous multicell activation in 3Ds, scanning microscopes can be modified to include a SLM to multiplex the beam prior to the scan via 3D-CGH (Packer et al., 2012; Yang et al., 2018). The holographic pattern, consisting of multiple near-diffraction limited spots ($\sim 1 \mu\text{m}$ in diameter), is then scanned in spiral trajectories on an area covering the size of the cell soma (Rickgauer and Tank, 2009; Packer et al., 2015; Yang et al., 2018).

Studies using hybrid methods in all-optical configurations have so far used C1V1 as optogenetic actuator excited at 1040 nm (Packer et al., 2015; 20–80 mW per target, spirals of 20 ms, 80 MHz repetition rate laser; Yang et al., 2018; 2.2–6.0 mW per target, spirals of 20 ms, low-repetition rate amplified laser). For 3D manipulation of neurons specifically, there is currently only one study where investigators simultaneously photostimulated more than 80 neurons over $150 \mu\text{m}$ in depth in layer 2/3 of the mouse visual cortex, while simultaneously imaging the activity of the surrounding neurons with GCaMP6s (Yang et al., 2018). The authors photoactivated in three different planes in an axial range of $100 \mu\text{m}$ selected groups of somatostatin inhibitory interneurons, suppressing the response of nearby pyramidal neurons to visual stimuli in awake animals (6 mW per cell from a low-repetition rate laser, or $6 \text{ mW}/\mu\text{m}^2$, since the surface of the illumination spot in that case is about $1 \mu\text{m}^2$, illumination for 2.8 s with 175 continuously repeated spirals, each lasting ~ 16 ms).

Maximum Number of Excitation Targets

An estimate of the maximum possible number of targets to address with each approach in the framework of an all-optical experiment, presumes knowledge of the total light losses of an optical system from the laser source to the objective output, which can significantly vary from one system to another. Moreover, the power necessary per target used, can vary according to opsin type, expression level, cell health and activation depth. In general, power losses for parallel illumination methods mainly consist of losses on the SLM(s) and the diffraction grating used for TF. For hybrid methods losses are approximately 2–3 times less than those of parallel ones, since they are mainly due to the use of a single SLM. It has also been reported that parallel approaches need about twice the power used by a spiral scanned beam, to induce a neuronal response with the same properties in both cases (Picot et al., 2018; Yang et al., 2018). Thus, in principle, for the same laser source and systems carefully designed to minimize power losses, hybrid methods are supposed

to outmatch parallel ones about 4 times in the maximum number of cells possibly activated (without considering photodamage limits). From what is reported so far in literature, the maximum number of cells that have been simultaneously activated with parallel approaches is 50 neurons (Mardinly et al., 2018), while for hybrid methods this number is reported to be up to 80 (Yang et al., 2018). In the first case, the authors clearly state that they were limited by the available power of their laser system. However, current advances in laser technology can provide fiber amplified systems that deliver up to 60 W maximum average power, allowing for the possibility to greatly increase the above reported numbers.

A fundamental difference between parallel and hybrid 3D multi-target photoactivation methods is the eventual photodamage effects that one can induce by increasing the number of targets and thus the amount of light that is sent to the tissue. As presented in the previously reported cases, in general, parallel illumination approaches use lower illumination intensity [$< 0.4 \text{ mW}/\mu\text{m}^2$ independently on the opsin type, see also (Chen et al., 2018b)] but higher total average power per target (e.g., for 2P *in vivo* activation 10–45 mW when amplified laser pulses of tens of μJ pulse energy are used from low-repetition rate fiber amplifiers, 30–90 mW when nJ-energy pulses are used from MHz-repetition rate oscillators) than scanning approaches (Chen et al., 2018b; Forli et al., 2018; Mardinly et al., 2018), making them more vulnerable to heating, i.e., linear photodamage. On the other hand, scanning (or hybrid) methods use high intensity ($2\text{--}6 \text{ mW}/\mu\text{m}^2$) focused beams of low total average power (Yang et al., 2018) (although average powers in the range of 20–80 mW were reported (Packer et al., 2015) when nJ-energy pulses were used from MHz-repetition rate oscillators), making them vulnerable to non-linear photodamage.

For non-linear photodamage, the damage threshold was shown to be inversely proportional to the pulse duration and proportional to the square of the mean power (König et al., 1999). It has been evaluated on the basis of morphological damage for CHO (Chinese Hamster Ovarian) cells to $0.1 \text{ J}/\text{cm}^2$ (König et al., 1999), or tissue ablation for porcine cornea (Olivié et al., 2008) to $1.5\text{--}2.2 \text{ J}/\text{cm}^2$ for 800–1000 nm. For comparison, an intensity of $80 \text{ mW}/\mu\text{m}^2$ at 80 MHz pulse repetition rate corresponds to a fluence of $0.1 \text{ J}/\text{cm}^2$. No relevant studies exist for the mouse brain. A recent study on tissue heating, took the standard illumination parameters for either parallel or scanning methods into consideration, showing that the local temperature rise on a target area did not exceed the physiological limits in both cases ($< 1 \text{ K}$) (Picot et al., 2018). Specifically, to generate an action potential *in vivo*, with a holographic spot of $12\text{-}\mu\text{m}$ diameter at a depth of $\sim 150 \mu\text{m}$, illuminating a neuron for 3 ms, at 1030 nm and $0.1 \text{ mW}/\mu\text{m}^2$, the average temperature rise over the spot's surface, is estimated to 0.3 K. Furthermore, comparing the temperature rise for experimental conditions able to generate action potentials with latency in the range of 2–10 ms *in vitro*, it was found that for a holographic spot (3-ms illumination, $0.2 \text{ mW}/\mu\text{m}^2$) the average rise was 1 K, while for a focused beam in a spiral trajectory (3-ms illumination, $31 \text{ mW}/\mu\text{m}^2$) the mean temperature rise was $< 0.5 \text{ K}$, and the local rise at the center

of the spiral was again ~ 1 K (Picot et al., 2018). For multi-target excitation, what remains critical is the distance between the different targets: for spots placed at an average distance from their nearest neighbor greater than the thermal diffusion length in tissue $\ell_{th} = \sqrt{6Dt}$, where D is the thermal diffusion constant [$140 \mu\text{m}^2/\text{ms}$ (Yizhar et al., 2011), and t the evolved time], the temperature rise remains comparable to the case of the isolated spot (for 3-ms illumination duration, holographic stimulation at an intensity $\leq 0.2 \text{ mW}/\mu\text{m}^2$ enables keeping the induced temperature rise < 2 K for activating 100 cells whose inter-soma distance was larger than the thermal diffusion length, which in that case was $\sim 50 \mu\text{m}$). Otherwise, the heat load starts to significantly increase locally (Picot et al., 2018). Moreover, in terms of illumination duration, prolonged stimulation (> 1 min) was found to induce substantial brain heating ($6\text{--}8^\circ\text{C}$) (Mardinly et al., 2018).

Notably, the considerations of the study by Picot et al. (2018) indicate that the optimal laser repetition rate for 2P optogenetics depends on the adopted illumination method: the very low excitation intensity used in parallel illumination, allows to neglect non-linear damage effects and privileges using low (500 kHz–2 MHz) repetition rate lasers to minimize heating through linear absorption. Scanning approaches on the other hand, require high excitation intensity but enable more efficient heat dissipation because of their small beam spot size; therefore, for short illumination times, a higher repetition rate laser (Ji et al., 2008) should be preferred in order to minimize peak-power-sensitive damages.

3D Imaging

In order to combine photostimulation and functional imaging over large neuronal populations in extended volumes, it is necessary to elaborate strategies to decouple and independently control the photostimulation and the imaging plane. An exhaustive presentation of the existing imaging techniques have recently been presented in literature (Ji et al., 2016; Yang and Yuste, 2017). Here we will discuss the techniques that can be combined with 3D photoactivation, in volumetric all-optical studies.

Adoption of approaches for 3D imaging, involving fast mechanical axial movements of the objective lens with piezoelectric positioners (Grewe et al., 2010; Katona et al., 2011), in combination with 3D photoactivation methods can be rather challenging for an independent control of the stimulation and imaging planes. In that case, the microscope objective is shared by both photostimulation and imaging paths, and a 3D all-optical configuration would require a simultaneous readjustment of the axial position of the photostimulation foci, to compensate for the objective shifts. Since 3D photoactivation methods use a SLM to project the excitation spots/patterns to different axial planes at a maximum refresh rate of 3 ms (Yang et al., 2016), a combination of fast piezo-repositioning approaches is feasible in cases where imaging is done in few discrete axial planes (Cossell et al., 2015; Peron et al., 2015; Seelig and Jayaraman, 2015), but not possible when objectives need to be moved over

an extended volume in a quasi-continuous way (Grewe et al., 2010; Katona et al., 2011).

Strategies involving the fast repositioning of the imaging focus by modulating the imaging beam divergence (**Figure 3A**), appear to be more convenient for all-optical volume investigations. This can be done by introducing a *lens-effect* in an upstream location of the imaging path, possibly in a plane conjugated to the objective back aperture to obtain a telecentric system. Clearly, the control of laser divergence must be fast enough to be compatible with functional imaging rates. Few technologies are commercially available for high-speed focus control through lenses. They are based either on the curvature change of a flexible-membrane electrically controlled lens (usually referred as Electrically Tunable Lens; ETL) (Grewe et al., 2011) or on ultrasounds propagating in a confined fluid, resulting in a tunable index of refraction gradient lens [usually referred as Tunable Acoustic Gradient (TAG) lens] that behaves like an aspheric lens (Mermillod-Blondin et al., 2008). ETLs have been mainly driven in stepping mode, enabling a ≈ 15 ms refocus time and can be electronically synchronized with the two-photon scanning imaging acquisition (Grewe et al., 2011). They have been successfully applied in 3D all-optical experiments, enabling simultaneous two-photon imaging and photostimulation on three planes axially spanning over $100 \mu\text{m}$ in mammals (Yang et al., 2018) and on five planes axially spanning over $32 \mu\text{m}$ in zebrafish (Dal Maschio et al., 2017). In TAG varifocal lenses, the optical power varies continuously at resonant frequencies, thus enabling much higher speeds with a $\approx 1 \mu\text{s}$ switching time, but they require careful control of oscillations through optical-phase locking (Kong et al., 2015). Volume imaging is built up by stacks of xz planes (where the fast-axis is along the axial direction) resulting in high-rate volume imaging ranging between 14 Hz ($375 \times 112 \times 130 \mu\text{m}^3$) and 56 Hz ($60 \times 4 \times 30 \mu\text{m}^3$).

Alternatively, SLMs or AODs can be used to dynamically control the degree of divergence of the imaging beam. SLM permits wavefront modulation resulting in fast beam refocusing (Dal Maschio et al., 2011) with refreshing rates up to 300 Hz. Importantly, in this case modulation is not limited to beam refocusing but can potentially be combined with more complex wavefront modulations, to correct optical aberrations (Booth, 2014) or to optimize the signal to noise ratio by targeting illumination of the cell (in this latter case in a CCD detection scheme) (Foust et al., 2015; Bovetti et al., 2017; Tanese et al., 2017). In the latter 2P near diffraction-limited stationary laser spots generated through CGH were used to perform scanless high-speed imaging of GCaMP6 activity in neurons *in vivo* on a CCD camera (Bovetti et al., 2017), or voltage imaging on dendritic spines (Tanese et al., 2017). CGH-shaped excitation was also used to improve the signal to noise ratio in voltage imaging experiments of dendrites and axons (Foust et al., 2015).

AODs can also be used for fast 3D beam repositioning. Using two pairs of orthogonal AODs addressed with counter-propagating acoustic waves of linearly varying frequency (chirped waves), it is possible to impress a precise xy radial deflection (determined by the center frequencies of the waves) and z axial displacement (determined by the amount of chirp) to the

illumination beam. Being completely inertia-free, AOD systems can achieve very short commutation (24.5 μs for 3D random access) and dwell (0.05–1.0 μs) times (Kirkby et al., 2010; Nadella et al., 2016). This makes AODs especially well-suited for high-rate random access point- or line-scanning imaging. For instance, in (Katona et al., 2012) the authors recorded responses from a population of individual neurons and glial cells, in the visual cortex of adult anesthetized mice, by automated tissue-drift compensation performed plane by plane, when obtaining a reference z-stack or between 3D random-access scans. They recorded spontaneous activity within $400 \times 400 \times 500 \mu\text{m}^3$ at a frequency up to 56 Hz. In another example (Nadella et al., 2016), researchers performed random-access patch imaging of neurons in layer 2/3 of primary visual cortex in an awake behaving mouse at 50 Hz, as well as the simultaneous dendritic and somatic imaging of pyramidal neurons in the visual cortex of awake mice at 27.9 Hz, by applying *post hoc* movement correction of images. The downside of such systems is that the combination of four AODs in a series is associated with power losses up to 75% (Reddy et al., 2008; Nadella et al., 2016) and requires strategies to compensate the temporal and spatial dispersion (Katona et al., 2012). However, recent developments in the AOD technology allow more efficient and uniform light transmission over larger scan angles when focusing away from the nominal focal plane of the objective (Nadella et al., 2016).

Remote focusing is another approach enabling fast sequential imaging of axially separated planes. It allows remote axial shifting the imaging beam by integrating a classical raster scanning system with an axial scan unit, which comprises of an objective lens and a lightweight mirror (Botcherby et al., 2007, 2012). Since the mirror is imaged on the sample plane, its oscillations are translated in a rapid change of focus in the sample, without physically moving the imaging objective lens. Fast oscillations are enabled by using a custom-built actuator constructed with a pair of galvanometer motors to scan the mirror in the kHz range. Importantly, as the two objectives are disposed to modify the beam wavefront with equal and opposite aberrations, the microscope is resilient to the systematic aberrations introduced by diverging beams that yield large focus shifts. Remote focusing enabled volume imaging of extracellular electrically induced calcium transients in OGB-loaded neurons up to 1 kHz, over a depth of 60 μm (Botcherby et al., 2012). Of note, other systems using remote focusing units, have used voice coil motors to drive the movable mirror at high speed (Rupprecht et al., 2016; Sofroniew et al., 2016).

Other volume imaging approaches, potentially compatible with 3D photostimulation, are based on multi-foci beams sent in parallel on the sample, imaging different planes simultaneously (Figure 3B), provided that *ad hoc* read-out demultiplexing strategies are adopted, to distinguish the signal coming from those planes. One possible strategy involves temporally multiplexed beams. Pulsed beams can be sent at different foci with different time delays. If the delays are superior to the fluorescence lifetime decay (in the range of few ns) and inferior to the inter-pulse interval, the fluorescence signal originating from different locations, can be distinguished by temporally demultiplexing the detected signal (Amir et al., 2007;

Cheng et al., 2011). Other strategies rely on computational demultiplexing algorithms, which permit simultaneous multi-foci imaging, without introducing any temporal shifts among the beams. In this case, a priori knowledge of the cells distribution and sparsity of cortical neuronal activity, allow demixing signals from different planes, using independent component analysis or non-negative matrix factorization algorithms (Yang et al., 2016).

Further strategies use extended depth of field (EDF) imaging, where the illumination PSF elongates axially (Botcherby et al., 2006). Since several layers of cells are encompassed within the PSF (Figure 3C), a lateral scan of such a beam is equivalent to projecting a stack of axially displaced layers in a single plane. Volume imaging is thus enabled at speeds equal to scan-based planar imaging. Very high-volume rates of functional imaging can thus be obtained, provided that neural activity comes from the sparse distribution of neurons, that do not significantly overlap axially and an *a priori* high-resolution mapping of the cells position in the volume, is acquired. Bessel beam based EDF functional volume imaging has been reported *in vivo* at 30 Hz for volumes extending up to 160 μm (Lu et al., 2017).

EDF imaging can also be obtained by engineering the detection PSF. Here, the strategy is conceptually reversed compared to previous approaches: instead of attaining volume imaging by modifying the illumination beam, axial discrimination is achieved by modulating the detected fluorescent signal. Similar to the excitation PSF, the detection PSF can be phase-only modulated with a transparent static phase mask placed at a Fourier plane of the detection path, so that it does not disturb the numerical aperture and the photon throughput of the system (no photon losses). Imaging can then be performed with a CCD and computational tools can be used to recover image information over the entire extended depth of field, as in the case of the elongated excitation PSF. Researchers have shown that the use of cubic phase masks in such configurations, in combination with CGH-based target illumination, allows for simultaneous imaging of fluorescence signals arising from different 3D targeted points (Quirin et al., 2013). Moreover, an *a priori* information of the origin of the fluorescence signal, through targeted excitation with CGH spots, can remove any ambiguity arising from imaging unknown objects with extended axial features (Quirin et al., 2013). Here, the strategy is conceptually reversed compared to previous approaches: instead of attaining volume imaging by modifying the illumination beam, axial discrimination is achieved by modulating the detected fluorescent signal.

Alternatively, volumetric imaging can be obtained in a wide-field illumination configuration using Light Field Microscopy (LFM) (Broxton et al., 2013) (Figure 3D). A series of micro lenses are placed at the native image plane (i.e., the plane where a camera is put in standard wide-field configurations) and a relay lens system is used to reimpose the lenslets' back focal plane onto a camera (Broxton et al., 2013). Since in-focus and out-of-focus light results in different patterns at the camera, axial localization of the emitters in a sample volume can be obtained by computationally processing the image. The volumetric imaging speed

is only limited by the CCD acquisition rate. Despite the high temporal performances, the application of LFM has been restricted to semi-transparent tissues due to scattering limitations (Broxton et al., 2013; Cohen et al., 2014; Prevedel et al., 2014). However, it has recently been proposed in a computational imaging approach, where it is integrated with high-dimensional, structured statistics enabling fast volumetric acquisition *in vivo* in the brains of mammals (Grosenick et al., 2017). If coupled with 3D photoactivation, particular attention needs to be paid when considering photoactivation cross-talk, as contamination induced by a single-photon wide-field imaging beam, may not be negligible.

Finally, light-sheet microscopy (LSM) represents another volumetric imaging approach (Figure 3E) particularly suited to whole-brain imaging of small-scale organisms (Keller and Ahrens, 2015; Power and Huisken, 2017), at single-cell imaging resolution (Ahrens et al., 2013). In this case, optical sectioning of the specimen is obtained in a conventional wide-field detection scheme, with an orthogonal illumination of the sample by means of a thin “sheet” of light coming from the side. Since excitation only yields in an axially confined planar portion of the sample, optically sectioned video-rate imaging of specific planes is enabled simply by using a common camera-based detection. 3D photostimulation coupling could be, e.g., envisaged by delivering photostimulation light through the high-NA detection objective. All-optical 3D functional investigations might then be obtained by adopting those LSM volumetric strategies involving axial light-sheet repositioning and varifocal ETL-based detection (Fahrbach et al., 2013) or cubic phase-based extended depth of field detection approaches, combined with imaging deconvolution (Olarde et al., 2015; Quirin et al., 2016). It is worth mentioning that, since the side-on light-sheet needs to uniformly excite a large portion of tissue, LSM is chiefly adopted for imaging of low-scattering media, even if imaging in relatively opaque tissues have been demonstrated in double-sided illumination and detection arrangements (Tomer et al., 2012; Lemon et al., 2015; Ezpeleta et al., 2016). Interestingly, double-sided illumination can be potentially used with one low-NA objective to generate the light-sheet and the other opposite-sided objective chosen with a high NA to address the 3D photostimulation patterns. At last, it should also be considered, that the orthogonal disposition of illumination and detection objectives, ultimately limit the geometric accessibility to the sample compared to other techniques relying on a single objective.

REFERENCES

- Accanto, N., Molinier, C., Tanese, D., Ronzitti, E., Newman, Z. L., Wyart, C., et al. (2018). Multiplexed temporally focused light shaping for high-resolution multi-cell targeting. *Optica* 5, 1478–1491. doi: 10.1364/OPTICA.5.001478
- Ahrens, M. B., Orger, M. B., Robson, D. N., Li, J. M., and Keller, P. J. (2013). Whole-brain functional imaging at cellular resolution using light-sheet microscopy. *Nat. Methods* 10, 413–420. doi: 10.1038/nmeth.2434
- Airan, R. D., Thompson, K. R., Fenno, L. E., Bernstein, H., and Deisseroth, K. (2009). Temporally precise *in vivo* control of intracellular signalling. *Nature* 458, 1025–1029. doi: 10.1038/nature07926

OUTLOOK

From this overview of the methods for 3D photoactivation and imaging, it is evident that these domains have tremendously advanced over the last few years. However, the combination of all-optical approaches is so far limited to use 2P scanning imaging modalities with an ETL (Dal Maschio et al., 2017; Mardinly et al., 2018; Yang et al., 2018), which is the most straightforward method for multiplane imaging, from those presented.

Nevertheless, the first steps have now been completed and we are entering an era where there will be an increasing demand for high-performance all-optical methods to tackle more complex biological questions. This will certainly prompt further developments for all-optical strategies in large excitation volumes and multi-area microscopes, where it will be possible, for instance, to activate a population of neurons in one area while monitoring the effects in another area of the brain (Lecoq et al., 2014; Chen et al., 2016). Furthermore, for imaging and photoactivation in large depths, development of micro-endoscopes based on miniaturized optics (Zong et al., 2017; Zou et al., 2017; Ozbay et al., 2018), able to perform all-optical manipulations, and use of three-photon excitation (Horton et al., 2013; Chen et al., 2018a; Rodríguez et al., 2018), can be envisioned.

AUTHOR CONTRIBUTIONS

EP conceived and organized the structure of the manuscript. EP and ER wrote the manuscript and prepared the figures. VE revised and contributed in writing the manuscript.

FUNDING

EP acknowledges the “Agence Nationale de la Recherche” ANR (Grants ANR-15-CE19-0001-01, 3DHoloPac) for financial support. ER acknowledges the European Research Council SYNERGY Grant Scheme (HELMHOLTZ, ERC Grant Agreement # 610110). VE acknowledges the National Institutes of Health (NIH) (1UF1NS107574-01), Human Frontier Science Program (HFSP) (RGP0015/2016), Fondation Bettencourt Shueller (Prix Coups d’Élan pour la Recherche Française) and AXA Research Fund.

- Amir, W., Carriles, R., Hoover, E. E., Durfee, C. G., and Squier, J. A. (2007). Simultaneous imaging of multiple focal planes in scanning two-photon absorption microscope. *Opt. Lett.* 32, 1731–1733. doi: 10.1117/12.731868
- Andrasfalvy, B. K., Zemelman, B. V., Tang, J., and Vaziri, A. (2010). Two-photon single-cell optogenetic control of neuronal activity by sculpted light. *Proc. Natl. Acad. Sci. U.S.A.* 107, 11981–11986. doi: 10.1073/pnas.1006620107
- Anselmi, F., Ventalon, C., Begue, A., Ogden, D., Emiliani, V., Bègue, A., et al. (2011). Three-dimensional imaging and photostimulation by remote-focusing and holographic light patterning. *Proc. Natl. Acad. Sci. U.S.A.* 108, 19504–19509. doi: 10.1073/pnas.1109111108
- Bañas, A., and Glückstad, J. (2017). Holo-GPC: holographic generalized phase contrast. *Opt. Commun.* 392, 190–195. doi: 10.1016/j.optcom.2017.01.036

- Bañas, A., Palima, D., Villangca, M., Aabo, T., and Glückstad, J. (2014). GPC light shaper for speckle-free one- and two-photon contiguous pattern excitation. *Opt. Express* 22, 5299–5310. doi: 10.1364/OE.22.005299
- Becker, Y., Unger, E., Fichte, M. A. H., Gacek, D. A., Dreu, A., Wachtveitl, J., et al. (2018). A red-shifted two-photon-only caging group for three-dimensional photorelease. *Chem. Sci.* 9, 2797–2802. doi: 10.1039/C7SC05182D
- Bègue, A., Papagiakoumou, E., Leschem, B., Conti, R., Enke, L., Oron, D., et al. (2013). Two-photon excitation in scattering media by spatiotemporally shaped beams and their application in optogenetic stimulation. *Biomed. Opt. Express* 4, 2869–2879. doi: 10.1364/BOE.4.002869
- Booth, M. J. (2014). Adaptive optical microscopy: the ongoing quest for a perfect image. *Light Sci. Appl.* 3:e165. doi: 10.1038/lsa.2014.46
- Botcherby, E. J., Juskaitis, R., Booth, M. J., and Wilson, T. (2007). Aberration-free optical refocusing in high numerical aperture microscopy. *Opt. Lett.* 32, 2007–2009. doi: 10.1364/OL.32.002007
- Botcherby, E. J., Smith, C. W., Kohl, M. M., Débarre, D., Booth, M. J., Juskaitis, R., et al. (2012). Aberration-free three-dimensional multiphoton imaging of neuronal activity at kHz rates. *Proc. Natl. Acad. Sci. U.S.A.* 109, 2919–2924. doi: 10.1073/pnas.1111662109
- Botcherby, E. J., Juskaitis, R., Wilson, T., Botcherby, E. J., Jus, R., Juskaitis, R., et al. (2006). Scanning two-photon fluorescence microscopy with extended depth of field. *Opt. Commun.* 268, 253–260. doi: 10.1016/j.optcom.2006.07.026
- Bovetti, S., Moretti, C., Zucca, S., Dal Maschio, M., Bonifazi, P., and Fellin, T. (2017). Simultaneous high-speed imaging and optogenetic inhibition in the intact mouse brain. *Sci. Rep.* 7:40041. doi: 10.1038/srep40041
- Broxton, M., Grosenick, L., Yang, S., Cohen, N., Andalman, A., Deisseroth, K., et al. (2013). Wave optics theory and 3-D deconvolution for the light field microscope. *Opt. Express* 21, 25418–25439. doi: 10.1364/OE.21.025418
- Carrillo-reid, L., Yang, W., Bando, Y., Peterka, D. S., and Yuste, R. (2016). Imprinting and recalling cortical ensembles. *Science* 353, 691–694. doi: 10.1126/science.aaf7560
- Carroll, E. C., Berlin, S., Levitz, J., Kienzler, M. A., Yuan, Z., Madsen, D., et al. (2015). Two-photon brightness of azobenzene photoswitches designed for glutamate receptor optogenetics. *Proc. Natl. Acad. Sci. U.S.A.* 112, E776–E785. doi: 10.1073/pnas.1416942112
- Chaigneau, E., Ronzitti, E., Gajowa, A. M., Soler-Llavina, J. G., Tanese, D., Brureau, Y. B. A., et al. (2016). Two-photon holographic stimulation of ReaChR. *Front. Cell. Neurosci.* 10:234. doi: 10.3389/fncel.2016.00234
- Chen, B., Huang, X., Gou, D., Zeng, J., Chen, G., Pang, M., et al. (2018a). Rapid volumetric imaging with Bessel-Beam three-photon microscopy. *Biomed. Opt. Express* 9, 1992–2000. doi: 10.1364/BOE.9.001992
- Chen, I. W., Papagiakoumou, E., and Emiliani, V. (2018b). Towards circuit optogenetics. *Curr. Opin. Neurobiol.* 50, 179–189. doi: 10.1016/j.conb.2018.03.008
- Chen, I.-W., Ronzitti, E., Lee, R. B., Daigle, L. T., Zeng, H., Papagiakoumou, E., et al. (2018c). Parallel holographic illumination enables sub-millisecond two-photon optogenetic activation in mouse visual cortex in vivo. *bioRxiv* [Preprint]. doi: 10.1101/250795
- Chen, J. L., Voigt, F. F., Javadzadeh, M., Krueppel, R., and Helmchen, F. (2016). Long-Range population dynamics of anatomically defined neocortical networks. *eLife* 5:e14679. doi: 10.7554/eLife.14679
- Cheng, A., Gonçalves, J. T., Golshani, P., Arisaka, K., and Portera-Cailliau, C. (2011). Simultaneous two-photon calcium imaging at different depths with spatiotemporal multiplexing. *Nat. Methods* 8, 139–142. doi: 10.1038/nmeth.1552
- Cohen, N., Yang, S., Andalman, A., Broxton, M., Grosenick, L., Deisseroth, K., et al. (2014). Enhancing the performance of the light field microscope using wavefront coding. *Opt. Express* 22, 24817–24839. doi: 10.1364/OE.22.024817
- Cossell, L., Iacaruso, M. F., Muir, D. R., Houlton, R., Sader, E. N., Ko, H., et al. (2015). Functional organization of excitatory synaptic strength in primary visual cortex. *Nature* 518, 399–403. doi: 10.1038/nature14182
- Dal Maschio, M., De Stasi, A. M., Benfenati, F., and Fellin, T. (2011). Three-dimensional in vivo scanning microscopy with inertia-free focus control. *Opt. Lett.* 36, 3503–3505. doi: 10.1364/OL.36.003503
- Dal Maschio, M., Difato, F., Beltramo, R., Blau, A., Benfenati, F., and Fellin, T. (2010). Simultaneous two-photon imaging and photo-stimulation with structured light illumination. *Opt. Express* 18, 18720–18731. doi: 10.1364/OE.18.018720
- Dal Maschio, M., Donovan, J. C., Helmbrecht, T. O., and Baier, H. (2017). Linking neurons to network function and behavior by two-photon holographic optogenetics and volumetric imaging. *Neuron* 94, 774–789.e5. doi: 10.1016/j.neuron.2017.04.034
- Dana, H., and Shoham, S. (2012). Remotely scanned multiphoton temporal focusing by axial grism scanning. *Opt. Lett.* 37, 2913–2915. doi: 10.1364/OL.37.002913
- Di Leonardo, R., Ianni, F., and Ruocco, G. (2007). Computer generation of optimal holograms for optical trap arrays. *Opt. Express* 15, 1913–1922. doi: 10.1364/OE.15.001913
- Ducros, M., Goulam Houssen, Y., Bradley, J., de Sars, V., and Charpak, S. (2013). Encoded multisite two-photon microscopy. *Proc. Natl. Acad. Sci. U.S.A.* 110, 13138–13143. doi: 10.1073/pnas.1307818110
- Durst, M. E., Zhu, G., and Xu, C. (2006). Simultaneous spatial and temporal focusing for axial scanning. *Opt. Express* 14, 12243–12254. doi: 10.1364/OE.14.012243
- Durst, M. E., Zhu, G., and Xu, C. (2008). Simultaneous spatial and temporal focusing in nonlinear microscopy. *Opt. Commun.* 281, 1796–1805. doi: 10.1016/j.optcom.2007.05.071
- Emiliani, V., Cohen, A. E., Deisseroth, K., and Häusser, M. (2015). All-optical interrogation of neural circuits. *J. Neurosci.* 35, 13917–13926. doi: 10.1523/JNEUROSCI.2916-15.2015
- Ezpeleta, E., Zurutuza, U., and Hidalgo, J. M. G. (2016). Using personality recognition techniques to improve Bayesian spam filtering. *Proces. Leng. Nat.* 57, 125–132. doi: 10.1038/nmeth.2064
- Fahrbach, F., Voigt, F., Schmid, B., Helmchen, F., and Huisken, J. (2013). Rapid 3D light-sheet microscopy with a tunable lens. *Opt. Express* 21, 1963–1975. doi: 10.1364/OE.21.021010
- Forli, A., Vecchia, D., Binini, N., Succol, F., Bovetti, S., Moretti, C., et al. (2018). Two-photon bidirectional control and imaging of neuronal excitability with high spatial resolution in vivo. *Cell Rep.* 22, 2809–2817. doi: 10.1016/j.celrep.2018.02.063
- Förster, D., Dal Maschio, M., Laurell, E., and Baier, H. (2017). An optogenetic toolbox for unbiased discovery of functionally connected cells in neural circuits. *Nat. Commun.* 8:116. doi: 10.1038/s41467-017-00160-z
- Foust, A. J., Zampini, V., Tanese, D., Papagiakoumou, E., and Emiliani, V. (2015). Computer-generated holography enhances voltage dye fluorescence discrimination in adjacent neuronal structures. *Neurophotonics* 2:021007. doi: 10.1117/1.NPh.2.2.021007
- Gerchberg, R. W., and Saxton, W. O. (1972). A practical algorithm for the determination of the phase from image and diffraction pictures. *Optik* 35, 237–246.
- Glückstad, J. (1996). Phase contrast image synthesis. *Opt. Commun.* 130, 225–230. doi: 10.1016/0030-4018(96)00339-2
- Go, M. A., Ng, P.-F., Bachor, H. A., and Daria, V. R. (2011). Optimal complex field holographic projection. *Opt. Lett.* 36, 3073–3075. doi: 10.1364/OL.36.003073
- Go, M. A., Stricker, C., Redman, S., Bachor, H.-A. A., and Daria, V. R. (2012). Simultaneous multi-site two-photon photostimulation in three dimensions. *J. Biophotonics* 5, 745–753. doi: 10.1002/jbio.201100101
- Göbel, N., Kampa, B. M., Helmchen, F., and Go, W. (2007). Imaging cellular network dynamics in three dimensions using fast 3D laser scanning. *Nat. Methods* 4, 73–79. doi: 10.1038/NMETH989
- Grewe, B. F., Langer, D., Kasper, H., Kampa, B. M., and Helmchen, F. (2010). High-speed in vivo calcium imaging reveals neuronal network activity with near-millisecond precision. *Nat. Methods* 7, 399–405. doi: 10.1038/nmeth.1453
- Grewe, B. F., Voigt, F. F., van 't Hoff, M., Helmchen, F., van 't Hoff, M., Helmchen, F., et al. (2011). Fast two-layer two-photon imaging of neuronal cell populations using an electrically tunable lens. *Biomed. Opt. Express* 2, 2035–2046. doi: 10.1364/BOE.2.002035
- Grosenick, L. M., Broxton, M., Kim, C. K., Liston, C., Poole, B., Yang, S., et al. (2017). Identification of cellular-activity dynamics across large tissue volumes in the mammalian brain. *bioRxiv* [Preprint]. doi: 10.1101/132688
- Guruge, C., Ouedraogo, Y. P., Comitz, R. L., Ma, J., Losonczy, A., and Nesnas, N. (2018). Improved synthesis of caged glutamate and caging each functional group. *ACS Chem. Neurosci.* 9, 2713–2727. doi: 10.1021/acscchemneuro.8b00152

- Haist, T., Schönleber, M., and Tiziani, H. (1997). Computer-generated holograms from 3D-objects written on twisted-nematic liquid crystal displays. *Opt. Commun.* 140, 299–308. doi: 10.1016/S0030-4018(97)00192-2
- Herlitze, S., and Landmesser, L. T. (2007). New optical tools for controlling neuronal activity. *Curr. Opin. Neurobiol.* 17, 87–94. doi: 10.1016/j.conb.2006.12.002
- Hernandez, O., Papagiakoumou, E., Tanese, D., Fidelin, K., Wyart, C., and Emiliani, V. (2016). Three-dimensional spatiotemporal focusing of holographic patterns. *Nat. Commun.* 7:11928. doi: 10.1038/ncomms11928
- Horton, N. G., Wang, K., Kobat, D., Clark, C. G., Wise, F. W., Schaffer, C. B., et al. (2013). In vivo three-photon microscopy of subcortical structures within an intact mouse brain. *Nat. Photonics* 7, 205–209. doi: 10.1038/nphoton.2012.336
- Isobe, K., Hashimoto, H., Suda, A., Kannari, F., Kawano, H., Mizuno, H., et al. (2010). Measurement of two-photon excitation spectrum used to photoconvert a fluorescent protein (Kaede) by nonlinear Fourier-transform spectroscopy. *Biomed. Opt. Express* 1, 687–693. doi: 10.1364/BOE.1.000687
- Ji, N., Freeman, J., and Smith, S. L. (2016). Technologies for imaging neural activity in large volumes. *Nat. Neurosci.* 19, 1154–1164. doi: 10.1038/nn.4358
- Ji, N., Magee, J. C., and Betzig, E. (2008). High-speed, low-photodamage nonlinear imaging using passive pulse splitters. *Nat. Methods* 5, 197–202. doi: 10.1038/nmeth.1175
- Katona, G., Kaszás, A., Turi, G. F., Hájós, N., Tamás, G., Vizi, E. S., et al. (2011). Roller Coaster Scanning reveals spontaneous triggering of dendritic spikes in CA1 interneurons. *Proc. Natl. Acad. Sci. U.S.A.* 108, 2148–2153. doi: 10.1073/pnas.1009270108
- Katona, G., Szalay, G., Maák, P., Kaszás, A., Veress, M., Hillier, D., et al. (2012). Fast two-photon in vivo imaging with three-dimensional random-access scanning in large tissue volumes. *Nat. Methods* 9, 201–208. doi: 10.1038/nmeth.1851
- Keller, P. J., and Ahrens, M. B. (2015). Visualizing whole-brain activity and development at the single-cell level using light-sheet microscopy. *Neuron* 85, 462–483. doi: 10.1016/j.neuron.2014.12.039
- Kim, E. H., Chin, G., Rong, G., Poskanzer, K. E., and Clark, H. A. (2018). Optical probes for neurobiological sensing and imaging. *Acc. Chem. Res.* 51, 1023–1032. doi: 10.1021/acs.accounts.7b00564
- Kirkby, P. A., Srinivas Nadella, K. M., and Silver, R. A. (2010). A compact Acousto-optic lens for 2D and 3D femtosecond based 2-photon microscopy. *Opt. Express* 18, 13721–13745. doi: 10.1364/OE.18.013720
- Klapoetke, N. C., Murata, Y., Kim, S. S., Pulver, S. R., Birdsey-Benson, A., Cho, Y. K., et al. (2014). Independent optical excitation of distinct neural populations. *Nat. Methods* 11, 338–346. doi: 10.1038/nmeth.2836
- Kong, L., Tang, J., Little, J. P., Yu, Y., Lämmermann, T., Lin, C. P., et al. (2015). Continuous volumetric imaging via an optical phase-locked ultrasound lens. *Nat. Methods* 12, 759–762. doi: 10.1038/nmeth.3476
- König, K., Becker, T. W., Fischer, P., Riemann, I., and Halbhauer, K.-J. (1999). Pulse-length dependence of cellular response to intense near-infrared laser pulses in multiphoton microscopes. *Opt. Lett.* 24, 113–115. doi: 10.1364/OL.24.000113
- Kwon, T., Sakamoto, M., Peterka, D. S., and Yuste, R. (2017). Attenuation of synaptic potentials in dendritic spines. *Cell Rep.* 20, 1100–1110. doi: 10.1016/j.celrep.2017.07.012
- Lecoq, J., Savall, J., Vuëinia, D., Grewe, B. F., Kim, H., Li, J. Z., et al. (2014). Visualizing mammalian brain area interactions by dual-axis two-photon calcium imaging. *Nat. Neurosci.* 17, 1825–1829. doi: 10.1038/nn.3867
- Lemon, W. C., Pulver, S. R., Höckendorf, B., McDole, K., Branson, K., Freeman, J., et al. (2015). Whole-central nervous system functional imaging in larval *Drosophila*. *Nat. Commun.* 6:7924. doi: 10.1038/ncomms8924
- Leshem, B., Hernandez, O., Papagiakoumou, E., Emiliani, V., and Oron, D. (2014). When can temporally focused excitation be axially shifted by dispersion? *Opt. Express* 22, 7087–7098. doi: 10.1364/OE.22.007087
- Levitz, J., Pantoja, C., Gaub, B., Janovjak, H., Reiner, A., Hoagland, A., et al. (2013). Optical control of metabotropic glutamate receptors. *Nat. Neurosci.* 16, 507–516. doi: 10.1038/nn.3346
- Liesener, J., Reicherter, M., Haist, T., and Tiziani, H. J. (2000). Multi-functional optical tweezers using computer-generated holograms. *Opt. Commun.* 185, 77–82. doi: 10.1016/S0030-4018(00)00990-1
- Lim, D., Chu, K. K., and Mertz, J. (2008). Wide-field fluorescence sectioning with hybrid speckle and uniform-illumination microscopy. *Opt. Lett.* 33, 1819–1821. doi: 10.1364/OL.33.001819
- Lu, R., Sun, W., Liang, Y., Kerlin, A., Bierfeld, J., Seelig, J. D., et al. (2017). Video-rate volumetric functional imaging of the brain at synaptic resolution. *Nat. Neurosci.* 20, 620–628. doi: 10.1038/nn.4516
- Lutz, C., Otis, T. S., DeSars, V., Charpak, S., Digregorio, D. A., and Emiliani, V. (2008). Holographic photolysis of caged neurotransmitters. *Nat. Methods* 5, 821–827. doi: 10.1038/nmeth.1241
- Mardinly, A. R., Oldenburg, I. A., Pégard, N. C., Sridharan, S., Lyall, E. H., Chesnov, K., et al. (2018). Precise multimodal optical control of neural ensemble activity. *Nat. Neurosci.* 21, 881–893. doi: 10.1038/s41593-018-0139-8
- Mermillod-Blondin, A., McLeod, E., and Arnold, C. B. (2008). High-speed varifocal imaging with a tunable acoustic gradient index of refraction lens. *Opt. Lett.* 33, 2146–2148. doi: 10.1364/OL.33.002146
- Nadella, K. M. N. S., Roš, H., Baragli, C., Griffiths, V. A., Konstantinou, G., Koimtzis, T., et al. (2016). Random access scanning microscopy for 3D imaging in awake behaving animals. *Nat. Methods* 13, 1001–1004. doi: 10.1038/nmeth.4033
- Nikolenko, V., Poskanzer, K. E., and Yuste, R. (2007). Two-photon photostimulation and imaging of neural circuits. *Nat. Methods* 4, 943–950. doi: 10.1038/NMETH1105
- Nikolenko, V., Watson, B. O., Araya, R., Woodruff, A., Peterka, D. S., and Yuste, R. (2008). SLM microscopy: scanless two-photon imaging and photostimulation with spatial light modulators. *Front. Neural Circuits* 2:5. doi: 10.3389/neuro.04.005.2008
- Olarte, O. E., Andilla, J., Artigas, D., and Loza-Alvarez, P. (2015). Decoupled illumination detection in light sheet microscopy for fast volumetric imaging. *Optica* 2, 702–705. doi: 10.1364/OPTICA.2.000702
- Olivé, G., Giguère, D., Vidal, F., Ozaki, T., Kieffer, J.-C., Nada, O., et al. (2008). Wavelength dependence of femtosecond laser ablation threshold of corneal stroma. *Opt. Express* 16, 4121–4129. doi: 10.1364/OE.16.004121
- Oron, D., Papagiakoumou, E., Anselmi, F., and Emiliani, V. (2012). Two-photon optogenetics. *Prog. Brain Res.* 196, 119–143. doi: 10.1016/B978-0-444-59426-6.00007-0
- Oron, D., Tal, E., and Silberberg, Y. (2005). Scanningless depth-resolved microscopy. *Opt. Express* 13, 1468–1476. doi: 10.1364/OPEX.13.001468
- Ozbay, B. N., Futia, G. L., Ma, M., Bright, V. M., Gopinath, J. T., Hughes, E. G., et al. (2018). Three dimensional two-photon imaging of neuronal activity in freely moving mice using a miniature fiber coupled microscope with active axial-scanning. *bioRxiv* [Preprint]. doi: 10.1101/226431
- Packer, A. M., Peterka, D. S., Hirtz, J. J., Prakash, R., Deisseroth, K., Yuste, R., et al. (2012). Two-photon optogenetics of dendritic spines and neural circuits. *Nat. Methods* 9, 1171–1179. doi: 10.1038/nmeth.2249
- Packer, A. M., Russell, L. E., Dalgleish, H. W. P., and Häusser, M. (2015). Simultaneous all-optical manipulation and recording of neural circuit activity with cellular resolution in vivo. *Nat. Methods* 12, 140–146. doi: 10.1038/nmeth.3217
- Papagiakoumou, E. (2013). Optical developments for optogenetics. *Biol. Cell* 105, 443–464. doi: 10.1111/boc.201200087
- Papagiakoumou, E., Anselmi, F., Bègue, A., de Sars, V., Glückstad, J., Isacoff, E. Y., et al. (2010). Scanless two-photon excitation of channelrhodopsin-2. *Nat. Methods* 7, 848–854. doi: 10.1038/nmeth.1505
- Papagiakoumou, E., Bègue, A., Leshem, B., Schwartz, O., Stell, B. M., Bradley, J., et al. (2013). Functional patterned multiphoton excitation deep inside scattering tissue. *Nat. Photonics* 7, 274–278. doi: 10.1038/nphoton.2013.9
- Papagiakoumou, E., de Sars, V., Oron, D., and Emiliani, V. (2008). Patterned two-photon illumination by spatiotemporal shaping of ultrashort pulses. *Opt. Express* 16, 22039–22047. doi: 10.1364/OE.16.022039
- Papagiakoumou, E., Ronzitti, E., Chen, I.-W., Gajowa, M., Picot, A., and Emiliani, V. (2018). Two-photon optogenetics by computer-generated holography. *Neuromethods* 133, 175–197. doi: 10.1007/978-1-4939-7417-7_10
- Pégard, N., Mardinly, A., Oldenburg, I., Waller, L., and Adesnik, H. (2018). *Partially Coherent Holographic temporal focusing for 3D light sculpting with single neuron resolution*. *Opt. InfoBase Conf. Pap. Part F88-B*, 4–5. doi: 10.1364/BRAIN.2018.BW2C.2.28^{}\$
- Pégard, N. M., Oldenburg, I., Sridharan, S., Waller, L., and Adesnik, H. (2017). 3D scanless holographic optogenetics with temporal focusing. *Nat. Commun.* 8:1228. doi: 10.1038/s41467-017-01031-3

- Peron, S. P., Freeman, J., Iyer, V., Guo, C., and Svoboda, K. (2015). A cellular resolution map of barrel cortex activity during tactile behavior. *Neuron* 86, 783–799. doi: 10.1016/j.neuron.2015.03.027
- Picot, A., Dominguez, S., Liu, C., Chen, I. W., Tanese, D., Ronzitti, E., et al. (2018). Temperature rise under two-photon optogenetic brain stimulation. *Cell Rep.* 24, 1243–1253.e5. doi: 10.1016/j.celrep.2018.06.119
- Piestun, R., Spektor, B., and Shamir, J. (1996). Wave fields in three dimensions: analysis and synthesis. *J. Opt. Soc. Am. A* 13, 1837–1848. doi: 10.1364/JOSAA.13.001837
- Power, R. M., and Huisken, J. (2017). A guide to light-sheet fluorescence microscopy for multiscale imaging. *Nat. Methods* 14, 360–373. doi: 10.1038/nmeth.4224
- Prakash, R., Yizhar, O., Grewe, B., Ramakrishnan, C., Wang, N., Goshen, I., et al. (2012). Two-photon optogenetic toolbox for fast inhibition, excitation and bistable modulation. *Nat. Methods* 9, 1171–1179. doi: 10.1038/nmeth.2215
- Prevedel, R., Verhoef, A. J., Pernía-Andrade, A. J., Weisenburger, S., Huang, B. S., Nöbauer, T., et al. (2016). Fast volumetric calcium imaging across multiple cortical layers using sculpted light. *Nat. Methods* 13, 1021–1028. doi: 10.1038/nmeth.4040
- Prevedel, R., Yoon, Y.-G., Hoffmann, M., Pak, N., Wetzstein, G., Kato, S., et al. (2014). Simultaneous whole-animal 3D imaging of neuronal activity using light-field microscopy. *Nat. Methods* 11, 727–730. doi: 10.1038/nmeth.2964
- Quirin, S., Peterka, D. S., and Yuste, R. (2013). Instantaneous three-dimensional sensing using spatial light modulator illumination with extended depth of field imaging. *Opt. Express* 21, 16007–16021. doi: 10.1364/OE.21.016007
- Quirin, S., Vladimirov, N., Yang, C.-T., Peterka, D. S., Yuste, R., and Ahrens, M. B. (2016). Calcium imaging of neural circuits with extended depth-of-field light-sheet microscopy. *Opt. Lett.* 41, 855–858. doi: 10.1364/OL.41.000855
- Reddy, G. D., Kelleher, K., Fink, R., and Saggau, P. (2008). Three-dimensional random access multiphoton microscopy for functional imaging of neuronal activity. *Nat. Neurosci.* 11, 713–720. doi: 10.1038/nn.2116
- Rickgauer, J. P., Deisseroth, K., and Tank, D. W. (2014). Simultaneous cellular-resolution optical perturbation and imaging of place cell firing fields. *Nat. Neurosci.* 17, 1816–1824. doi: 10.1038/nn.3866
- Rickgauer, J. P., and Tank, D. W. (2009). Two-photon excitation of channelrhodopsin-2 at saturation. *Proc. Natl. Acad. Sci. U.S.A.* 106, 15025–15030. doi: 10.1073/pnas.0907084106
- Rodríguez, C., Liang, Y., Lu, R., and Ji, N. (2018). Three-photon fluorescence microscopy with an axially elongated Bessel focus. *Opt. Lett.* 43, 1914–1917. doi: 10.1364/OL.43.001914
- Ronzitti, E., Conti, R., Zampini, V., Tanese, D., Foust, A. J., Klapoetke, N., et al. (2017a). Sub-millisecond optogenetic control of neuronal firing with two-photon holographic photoactivation of Chronos. *J. Neurosci.* 37, 10679–10689. doi: 10.1523/JNEUROSCI.1246-17.2017
- Ronzitti, E., Ventalon, C., Canepari, M., Forget, B. C., Papagiakoumou, E., and Emiliani, V. (2017b). Recent advances in patterned photostimulation for optogenetics. *J. Opt.* 19:113001. doi: 10.1088/2040-8986/aa8299
- Rupprecht, P., Prendergast, A., Wyart, C., and Friedrich, R. W. (2016). Remote z-scanning with a macroscopic voice coil motor for fast 3D multiphoton laser scanning microscopy. *Biomed. Opt. Express* 7, 1656–1671. doi: 10.1364/BOE.7.001656
- Seelig, J. D., and Jayaraman, V. (2015). Neural dynamics for landmark orientation and angular path integration. *Nature* 521, 186–191. doi: 10.1038/nature14446
- Shemesh, O. A., Tanese, D., Zampini, V., Linghu, C., Piatkevich, K., Ronzitti, E., et al. (2017). Temporally precise single-cell resolution optogenetics. *Nat. Neurosci.* 20, 1796–1806. doi: 10.1038/s41593-017-0018-8
- Sofroniew, N. J., Flickinger, D., King, J., and Svoboda, K. (2016). A large field of view two-photon mesoscope with subcellular resolution for in vivo imaging. *eLife* 5:e14472. doi: 10.7554/eLife.14472
- Stirman, J. N., Smith, I. T., Kudenov, M. W., and Smith, S. L. (2016). Wide field-of-view, multi-region, two-photon imaging of neuronal activity in the mammalian brain. *Nat. Biotechnol.* 34, 857–862. doi: 10.1038/nbt.3594
- Sun, B., Salter, P. S., Roider, C., Strauss, J., Heberle, J., and Booth, M. J. (2018). Four-dimensional light shaping?: manipulating ultrafast spatio-temporal foci in space and time. *Light Sci. Appl.* 7:17117. doi: 10.1038/lsa.2017.117
- Szabo, V., Ventalon, C., De Sars, V., Bradley, J., and Emiliani, V. (2014). Spatially selective holographic photoactivation and functional fluorescence imaging in freely behaving mice with a fiberscope. *Neuron* 84, 1157–1169. doi: 10.1016/j.neuron.2014.11.005
- Tanese, D., Weng, J.-Y., Zampini, V., De Sars, V., Canepari, M., Rozsa, B., et al. (2017). Imaging membrane potential changes from dendritic spines using computer-generated holography. *Neurophotonics* 4:031211. doi: 10.1117/1.NPh.4.3.031211
- Tomer, R., Khairy, K., Amat, F., and Keller, P. J. (2012). Quantitative high-speed imaging of entire developing embryos with simultaneous multiview light-sheet microscopy. *Nat. Methods* 9, 755–763. doi: 10.1038/nmeth.2062
- Vogt, N. (2015). All-optical electrophysiology in behaving animals. *Nat. Methods* 12:101. doi: 10.1038/nmeth.3272
- Yang, S., Papagiakoumou, E., Guillon, M., de Sars, V., Tang, C. M., and Emiliani, V. (2011). Three-dimensional holographic photostimulation of the dendritic arbor. *J. Neural Eng.* 8:46002. doi: 10.1088/1741-2560/8/4/046002
- Yang, W., Carrillo-reid, L., Bando, Y., Peterka, D. S., and Yuste, R. (2018). Simultaneous two-photon optogenetics and imaging of cortical circuits in three dimensions. *eLife* 7:e32671. doi: 10.7554/eLife.32671
- Yang, W., Miller, J. K., Carrillo-Reid, L., Pnevmatikakis, E., Paninski, L., Yuste, R., et al. (2016). Simultaneous multi-plane imaging of neural circuits. *Neuron* 89, 269–284. doi: 10.1016/j.neuron.2015.12.012
- Yang, W., and Yuste, R. (2017). In vivo imaging of neural activity. *Nat. Methods* 14, 349–359. doi: 10.1038/nmeth.4230
- Yang, W., and Yuste, R. (2018). Holographic imaging and photostimulation of neural activity. *Curr. Opin. Neurobiol.* 50, 211–221. doi: 10.1016/j.conb.2018.03.006
- Yizhar, O., Fenno, L. E., Davidson, T. J., Mogri, M., and Deisseroth, K. (2011). Optogenetics in neural systems. *Neuron* 71, 9–34. doi: 10.1016/j.neuron.2011.06.004
- Zhu, G., van Howe, J., Durst, M., Zipfel, W., and Xu, C. (2005). Simultaneous spatial and temporal focusing of femtosecond pulses. *Opt. Express* 13, 2153–2159. doi: 10.1364/OPEX.13.002153
- Zong, W., Wu, R., Li, M., Hu, Y., Li, Y., Li, J., et al. (2017). Fast high-resolution miniature two-photon microscopy for brain imaging in freely behaving mice. *Nat. Methods* 14, 713–719. doi: 10.1038/nmeth.4305
- Zou, Y., Chau, F. S., and Zhou, G. (2017). Ultra-compact optical zoom endoscope using solid tunable lenses. *Opt. Express* 25, 20675–20688. doi: 10.1364/OE.25.020675

Conflict of Interest Statement: The authors declare that the research was conducted in the absence of any commercial or financial relationships that could be construed as a potential conflict of interest.

The handling Editor declared a past co-authorship with the authors.

Copyright © 2018 Ronzitti, Emiliani and Papagiakoumou. This is an open-access article distributed under the terms of the Creative Commons Attribution License (CC BY). The use, distribution or reproduction in other forums is permitted, provided the original author(s) and the copyright owner(s) are credited and that the original publication in this journal is cited, in accordance with accepted academic practice. No use, distribution or reproduction is permitted which does not comply with these terms.